

Synthesis of new apatite phases by spray pyrolysis and their characterization

D. VEILLEUX, N. BARTHELEMY, J.-C. TROMBE, M. VERELST
*Centre d'Elaboration de Matériaux et d'Etudes Structurales, UPR8011,
 BP 4347, 29 rue Jeanne Marvig, 31055 Toulouse Cédex 4, France
 E-mail: verelst@cemes.fr*

This paper describes the synthesis of some apatite compounds, called britholites, by an aerosol pyrolysis technique, which compared to conventional methods of solid-state chemistry, presents the advantages of reducing noticeably the temperature and the duration of the treatment. Britholites are minerals based on $\text{Ca}_{10-x}\text{Ln}_x(\text{PO}_4)_{6-x}(\text{SiO}_4)_x\text{X}_2$ formula (with $X = \text{F}^-$, OH^- , $\text{X}_2 = \text{O}^{2-}$); they are promising materials for nuclear waste storage. In a second part we have synthesized and characterized a new apatite phase where the substitution of calcium by barium in britholite leads to a monophased solid solution $\text{Ca}_{9-x}\text{Ba}_x\text{Nd}(\text{PO}_4)_{6-x}(\text{SiO}_4)\text{F}_2$ for $6 < x < 9$. The possible interest of this new material is discussed. © 2001 Kluwer Academic Publishers

1. Introduction

In order to confine high level radioactive wastes produced by processing irradiated nuclear fuel, confinement inside solid matrices as glasses, glass-ceramics and crystalline ceramics has been intensively studied for several decades. Even if the “glass process” is now an industrial method [1] a lot of researches are still going on to find more durable materials. Several host inorganic matrices have been proposed such as zircon, monazite, thorium-phosphate, barium-phosphate, apatite [2–6]. Long-term storage requires a material able to immobilize these elements (like neptunium, americium and curium) for a long time (about 10^6 years). Among these matrices, our choice was apatite compounds. The durability of natural apatites is well demonstrated by the apatites from the Oklo (Gabon) natural reactor which have retained high fission-product elements in their structure despite exposure to the geologic environment for nearly 2 billion years [7]. Indeed, for some special composition these apatitic minerals, usually called britholite, can present a non-metamict behaviour [6]. Non-metamict means, that, at relative low temperature, (less than the storage temperature) the recovery rate of the structure is faster than the amorphisation phenomenon caused by the self-radioactive decomposition of the incorporated actinide. This last behaviour is a crucial advantage to consider britholite as the most promising matrix for nuclear waste storage.

Apatites are very common in nature: they occur in limited quantities in almost all igneous rocks, but they constitute also the mineral part of bone and teeth of vertebrate animals [8]. The term apatite refers to a group of minerals presenting the same basic structure (hexagonal system, space group $P6_3/m$) and the same general formula, $\text{M}_{10}(\text{XO}_4)_6\text{Y}_2$, where M, XO_4 and Y are generally a divalent cation (Ca. . .), a triva-

lent anion (PO_4 . . .) and a monovalent anion (F, OH. . .) respectively [9]. One of the interesting properties of the apatite structure is the extensive isomorphous substitution or charge-coupled substitution which occurs in it [10]. For example, M can be a lanthanide or an actinide; in this case the charge balance is provided either by the replacement of phosphate by silicate or by the replacement of fluoride ions by O^{2-} ones. The phosphate-silicate apatites are called britholites. Because of the similarities in the chemical features of lanthanide and actinide, the former ones have been chosen as models of britholite containing radioactive actinide. Such britholites, $\text{Ca}_{10-x}\text{Ln}_x(\text{PO}_4)_{6-x}(\text{SiO}_4)_x\text{F}_2$ and $\text{Ca}_{10-x}\text{Ln}_x(\text{PO}_4)_{6-x}(\text{SiO}_4)_x\text{O}\square$ with $0 \leq x \leq 6$ and $\text{Ln} = \text{La}, \text{Nd}$, have been prepared via solid state [11, 12]. The solid-state route requires high reaction temperatures (1400°C), long heating times and numerous grinding processes to obtain pure phases. Therefore, the particles obtained via this route are agglomerated particles of irregular shape which show poor sinterability.

Studies using the spray pyrolysis technique are relatively scarce. This method, starting with solutions that can be acidic, leads to homogeneous and stoichiometric materials. For example, it has been used to synthesize the calcium phosphate hydroxyapatite [13–16]. The resulting hydroxyapatite, mixed with a small amount of β -tricalcium phosphate, is composed of spherical particles with a diameter of about $1 \mu\text{m}$. In this paper, the spray pyrolysis method is used to prepare firstly the calcium phosphate hydroxyapatite and fluorapatite or their corresponding barium apatites and secondly the britholites, $\text{Ca}_{9-x}\text{Ba}_x\text{Nd}(\text{PO}_4)_{6-x}(\text{SiO}_4)\text{F}_2$ with $0 \leq x \leq 9$.

2. Experimental part

The spray pyrolysis apparatus is represented in Fig. 1. This apparatus consists of three different parts:

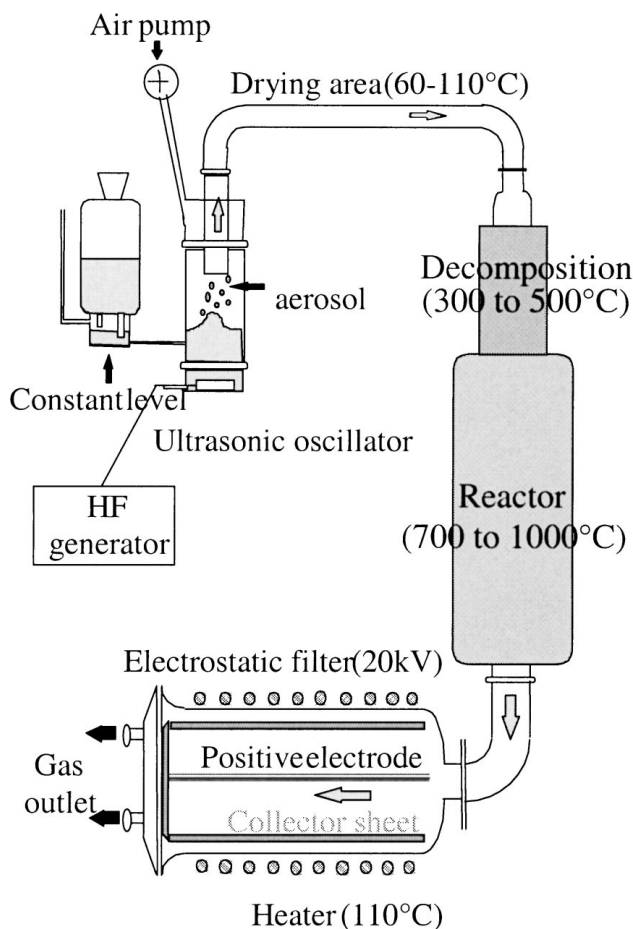


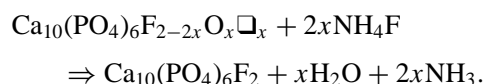
Figure 1 The spray pyrolysis process.

- the atomizer which forms an aerosol of thin droplets with the help of an ultrasonic oscillator with a frequency of 2.6 MHz. The droplet size mainly depends on the oscillator frequency, but also on the concentration and viscosity of the starting solution. The droplet size can roughly range from 2 to 5 μm [17]. As soon as droplets are formed, they are carried away by an air flow (5l/mn) to the next zones.
- the furnace zones, which are divided into three parts. First, the drying zone (60–110°C), where solvents are evaporated and where precursor salts precipitate. Secondly, the decomposition area (300–500°C), where precursor compounds are decomposed, and finally the reactor zone (700–1000°C), where solid state reactions take place and where the densification of particles begins. It is worthwhile noticing the very short time necessary for this process; in our conditions, the solid particles stay at the maximum temperature for a few seconds only.
- the collecting zone, where an electrostatic filter (20 KV) recovers most (60 to 80%) of the products. This electrostatic filter temperature is maintained around 110°C to prevent solvent condensation on the prepared compounds.

The tube where the reactions take place is made of pyrex-glass and of silica.

The starting reactants were chosen so that they will not precipitate in the solution. The metal elements were in the form of nitrates ($\text{Ca}(\text{NO}_3)_2 \cdot 4\text{H}_2\text{O}$, $\text{Ba}(\text{NO}_3)_2$, $\text{Nd}(\text{NO}_3)_3 \cdot 6\text{H}_2\text{O}$). The sources of phosphorus, silicon and fluorine were respectively triethylphosphate, tetramethylsilicate and trifluoroacetic acid. The reactants were weighed in order to reach the molar ratio of stoichiometric apatite, $\text{Ca} + \text{Ba} + \text{Nd}/(\text{PO}_4) + (\text{SiO}_4) = 1.67$. The reactants were dissolved in aqueous medium (320 ml distilled water and 80 ml methanol [18]). The concentration of the solution, $(\Sigma\text{Ca} + \text{Ba} + \text{Nd})$, was fixed at 0.1 M. The rough samples of the spray pyrolysis were annealed at different temperatures (1000°C–1300°C) for some hours.

Preliminary experiments carried out on $\text{Ca}_{10}(\text{PO}_4)_6\text{F}_2$ with a stoichiometric $\text{F}/(\text{PO}_4)$ atomic ratio equals to 1/3, reveal a fluoride deficiency. Therefore, this ratio was increased (1/3, 1/1 and 3/1). Even by using the latter concentration of fluoride ions, one can observe a slight deficiency of these ions in the resulting apatites. In this case, the proportion of the fluoride ions was increased by using an ion-exchange process, $\text{OH}^- \leftrightarrow \text{F}^-$ or $\text{O}^{2-} \leftrightarrow 2\text{F}^-$ realized at high temperature (800°C) under a stream of dry nitrogen [19]:



Fluoride titrations were performed by a specific electrode in aqueous medium. Powdered samples were dissolved in per-chloric acid and buffered with tri-sodium citrate (1 M).

The phases obtained were characterized particularly by X-ray diffraction powder using a Seifert XRD3000 diffractometer ($\text{Cu K}\alpha$ radiation). The crystalline phases were compared to the data on JCPDS cards. When different phases were observed, their relative amounts were determined by comparing the main X-ray reflections. The infrared spectra were obtained in a range from 400 to 4000 cm^{-1} on KBr pellets by using a Perkin-Elmer FT-IR 1725X.

3. Results and discussion

Before studying the preparation of britholites, we have decided to check our technique of spray pyrolysis on more simple apatites such as calcium phosphate hydroxyapatite and fluorapatite. Then these results will be extended to barium-apatites. Ba-apatites are generally less studied than their calcium counterparts.

3.1. Non substituted apatite compounds

3.1.1. Preparation and characterization of calcium apatite

The results of the synthesis of calcium hydroxyapatite (Hap) are summarized in Table I. The X-ray diffraction pattern (XRD) of the rough sample of the spray pyrolysis presents a mixture of different phases: $\text{Ca}_3(\text{PO}_4)_2$ (β -PTCa) (JCPDS card 09-0169), Hap (JCPDS card 09-0432 and CaO (JCPDS card 48-1467). β -PTCa is preponderant and Hap is poorly crystallized.

TABLE I Preparation of the hydroxyapatite: $(\text{Ca}_{10}(\text{PO}_4)_6(\text{OH})_2 = \text{Hap}$, $\beta\text{-PTCa} = \text{Ca}_3(\text{PO}_4)_2$ β -type)

	crude sample (rough spray- pyrolysed sample)	sample heated at 1000°C, for 12 hour
XRD observations	$\beta\text{-PTCa} > \text{Hap} > \text{CaO}$	$\text{Hap} > \beta\text{-PTCa} > \text{CaO}$ (traces)
	$a = 9.401(5) \text{ \AA}$	$a = 9.421(1) \text{ \AA}$
	$c = 6.895(5) \text{ \AA}$	$c = 6.884(1) \text{ \AA}$

The unit-cells of the apatite compound (rough sample) are different from those of stoichiometric Hap ($a = 9.418 \text{ \AA}$, $c = 6.884 \text{ \AA}$, JCPDS card 09-0432; $a = 9.421 \text{ \AA}$, $c = 6.883 \text{ \AA}$) [20]. The introduction of carbonate ions replacing the phosphate groups (B-type carbonate apatite) can be responsible for such differences [8, 21]. In addition to the phosphate group, the infrared spectrum of this compound shows some bands at 1420, 1455 and 870 cm^{-1} which are a signature of such substitution.

Hap becomes the main phase when the preceding sample is annealed at 1000°C in air atmosphere, for 1 or 12 hours, but it is always mixed with some $\beta\text{-PTCa}$ (about 30%) and CaO (traces) (Fig. 2). Such a heating treatment improves greatly the Hap crystallinity. The unit-cell constants of this last compound are comparable to the stoichiometric Hap ones (Table I). Fig. 3 shows the infrared spectra of the Hap and Fap apatites. Hap presents the bands assigned to the phosphate function ($1092, 1044, 966, 604$ and 576 cm^{-1}) and the bands attributed to the hydroxyl group (3570 and 632 cm^{-1}) [8, 20].

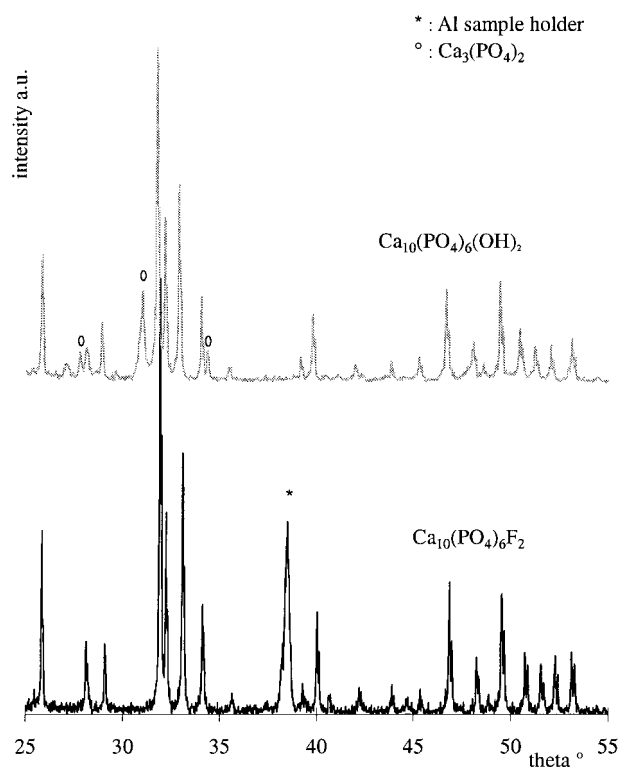


Figure 2 XRD patterns of Hap and Fap apatites after annealing at 1200°C under air for one hour.

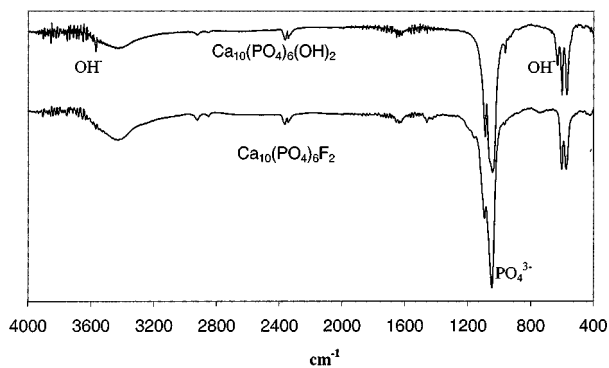


Figure 3 Infrared spectra of Hap and Fap apatites after annealing at 1200°C under air for one hour.

The preparation of the phosphocalcium fluorapatite (Fap) is given in Table II. The rough sample of Fap, obtained by spraying the reactants in stoichiometric composition ($\text{F}^-/\text{PO}_4^{3-} = 1/3$) presents several phases ($\beta\text{-PTCa} > \text{Fap} > \text{CaO}$). Annealing this product at 1200°C for one hour results in a decrease of $\beta\text{-PTCa}$ with an increase of the apatite phase which becomes well crystallized. However its unit-cell constants are quite different ($a = 9.389(2) \text{ \AA}$ and $c = 6.884(1) \text{ \AA}$) from those of stoichiometric Fap (JCPDS cards 15-0876, $a = 9.3684 \text{ \AA}$ and $c = 6.8841 \text{ \AA}$; or 75-0915, $a = 9.37(1) \text{ \AA}$ and $c = 6.88(1) \text{ \AA}$). In particular, the a parameter differs by 0.02 from the one of stoichiometric Fap. Such a variation can be the result of the replacement of some F^- ions by some O^{2-} or OH^- [19]. This deficiency of fluoride ions can be due to several reasons. First, the fluorine element, introduced as trifluoroacetic acid, could react with the silica tube to give gaseous SiF_4 , which may not have enough time to react with the forming apatite and may be carried away by the carrier gas. Secondly, some fluoride ions of the apatite could be lost during the heating treatment at high temperature. Thus, the starting concentration of trifluoroacetic acid has been increased by 3 times and by 9 times according to the stoichiometric proportions.

The increase of the $\text{F}^-/\text{PO}_4^{3-}$ starting ratio leads to an increase of the apatite phase compared to the proportion of $\beta\text{-PTCa}$. For $\text{F}^-/\text{PO}_4^{3-} = 3/1$, the Fap is the only phase even for the rough spray pyrolyzed sample. A chemical dosage of the fluoride ions on this last sample leads to about 90% of the stoichiometric proportion. Moreover, as soon as the $\text{F}^-/\text{PO}_4^{3-}$ ratio of the starting reactants is increased, the a unit-cell dimension of the samples, annealed at 1200°C for one hour, begins to decrease. And for $\text{F}^-/\text{PO}_4^{3-} = 3/1$, the unit-cell parameters are very close to those of stoichiometric Fap, particularly the a parameter. The XRD pattern of fluorapatite, obtained with $\text{F}^-/\text{PO}_4^{3-} = 3/1$ and annealed at 1200°C , is given in Fig. 2. The infrared spectrum of this sample is presented in Fig. 3. In addition to phosphate bands, this spectrum shows weak bands, $1150\text{--}1200 \text{ cm}^{-1}$ and 750 cm^{-1} , which are a signature of SiO_2 vibrations. The presence of such phases is in agreement with the reaction of fluoride on the silica tube.

In our conditions of spray pyrolysis, Ca-Hap can not be prepared as a pure phase. This result agrees with that of Aizawa [16]. It is likely that oxyhydroxyapatite

TABLE II Preparation of the phosphocalcium fluorapatite: $\text{Ca}_{10}(\text{PO}_4)_6\text{F}_2 = \text{Fap}$, $\beta\text{-PTCa} = \text{Ca}_3(\text{PO}_4)_2$ β -type)

$\text{F}^-/\text{PO}_4^{3-}$ Ratio	Rough spray-pyrolysed sample	Sample annealed at 1200°C, for 1 hour, under N_2	Cell constants of annealed samples	Cell volume
1/3	$\beta\text{-PTCa} > \text{Fap} > \text{CaO}$	$\text{Fap} > \beta\text{-PTCa} > \text{CaO}$	$a = 9.389(2) \text{ \AA}$ $c = 6.884(1) \text{ \AA}$	525.5 \AA^3
1/1	$\text{Fap} = \beta\text{-PTCa} > \text{CaO}$	Fap	$a = 9.3799(9) \text{ \AA}$ $c = 6.8864(7) \text{ \AA}$	524.7 \AA^3
3/1	Fap	Fap	$a = 9.3708(8) \text{ \AA}$ $c = 6.8876(7) \text{ \AA}$	523.8 \AA^3

was formed at the spray-pyrolysis temperature, 1000°C. This last apatite is unstable and is easily decomposed into $\beta\text{-PTCa}$ and CaO or $\beta\text{-PTCa}$ and tetracalcium phosphate [20, 22]. On the contrary, Ca-Fap can be prepared as a pure phase as soon as the $\text{F}^-/\text{PO}_4^{3-}$ ratio of the starting reactants is 9 times greater than the stoichiometric proportion. This possibility may be due to a competition between F^- and O^{2-} in the apatite forming at 1000°C.

3.1.2. Preparation and characterization of barium apatite

Ba-apatite was prepared in the same way as its corresponding calcium. The rough sample of Ba-Hap presents several phases: poorly crystallized apatite (JCPDS card, 36-0272), $\text{Ba}_3(\text{PO}_4)_2$ (JCPDS card 25-0028), $\text{Ba}_2\text{P}_2\text{O}_7$ (JCPDS card 30-0144) and BaCO_3 (JCPDS card 44-1487). After an annealing treatment at 1200°C for one hour under a nitrogen stream, the barium pyrophosphate and the barium carbonate disappear but several phases still remain: $\text{Ba}_3(\text{PO}_4)_2$ which is preponderant, well crystallized apatite and BaO (JCPDS card 30-0143). This thermal treatment induces a decrease of the intensity of the apatite. The lattice parameters of this last apatite ($a = 10.16(2) \text{ \AA}$ and $a = 7.76(2) \text{ \AA}$) are close to the values of Ba-Hap (JCPDS card, 36-0272; $a = 10.1912(4) \text{ \AA}$ and $a = 7.7470(4) \text{ \AA}$). The variation between these parameters can be explained by a O^{2-} substitution in the channel sites. Indeed, no OH^- vibration is noted in the infrared spectrum of this last apatite.

Our attempts to prepare the Ba-Fap have completely failed even by using an excess of fluoride ions in the starting reactants ($\text{F}^-/(\text{PO}_4)^{3-} = 3/1$). Neither in rough sample nor in the sample heated in the previous conditions (see Ba-Hap) any apatite phase is disclosed by XRD. For example, in the sample heated for one hour, a mixture of $\text{Ba}_2\text{P}_2\text{O}_7$ and BaO is observed. Increasing the time of this treatment up to 5 hours results in the same phases mixed with $\text{Ba}_3(\text{PO}_4)_2$. Unlike the calcium pyrophosphate, which shows a great reactivity when it is heated in the presence of CaO , the corresponding barium one is very stable in the presence of BaO . In our conditions of spray pyrolysis, Ba-apatites, either Hap or Fap, are more difficult to obtain than the calcium counterparts.

3.2. Preparation of substituted apatites (britholites)

The preparation of britholite will be carried out with a ratio of F^- to $(\text{PO}_4)^{3-} + (\text{SiO}_4)^{4-}$ equal to three. We

will study particularly the $\text{Ca}_9\text{Nd}(\text{PO}_4)_5(\text{SiO}_4)\text{F}_2$, and then the calcium element will be progressively replaced by the barium one.

3.2.1. Study of the $\text{Ca}_9\text{Nd}(\text{PO}_4)_5(\text{SiO}_4)\text{F}_2$

The rough spray-pyrolysed sample presents only one poorly crystallized apatite phase. By heating under an atmosphere of nitrogen for one hour at different temperatures, the crystallinity of this phase is increased, but this treatment leads to a modification of the unit-cell constants (Fig. 4). An annealing treatment at 1000°C results in a slight decrease of the volume, compared to the volume of the rough sample, but an increase of this treatment up to 1300°C leads to an increase of this volume. Several reasons can be suggested for the first decrease of this volume (see later, infrared analysis). As the temperature of the annealing treatment is increased up to 1300°C, the volume increase can be due to a decrease of fluoride ions. For example, the fluoride percentage equals 66.1% and 61.1% for a heating treatment at 1200°C and 1300°C respectively. This percentage of fluoride ions can be increased to 89.2%, if a post-fluoridation (ion-exchange process) treatment is performed, after the annealing treatment at 1200°C.

In spite of some imprecisions, the determination of the structure by X-ray diffraction (on powder) associated with Rietveld refinement on this last sample leads to the formula, $\text{Ca}_{9.2}\text{Nd}_{0.8}(\text{PO}_4)_{5.2}(\text{SiO}_4)_{0.8}\text{F}_{1.8}\text{O}_{0.1}\square_{0.1}$, which is close to the expected formula. Some O^{2-} atoms occur in the channel sites; a slight amount of these ions is required for charge balance. Although there are some neodymium atoms in the two cationic sites of the apatite structure, Rietveld

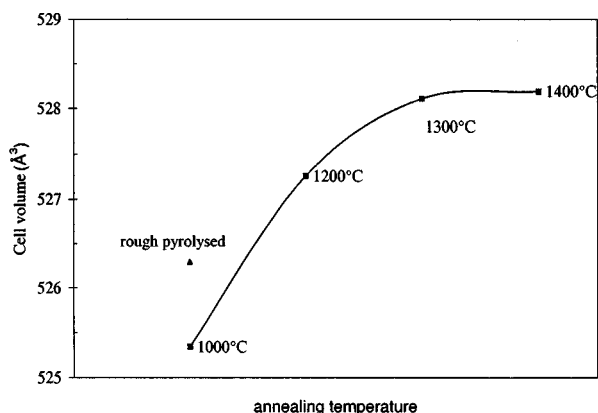


Figure 4 Evolution of the apatite volume cell versus the annealing temperature under nitrogen.

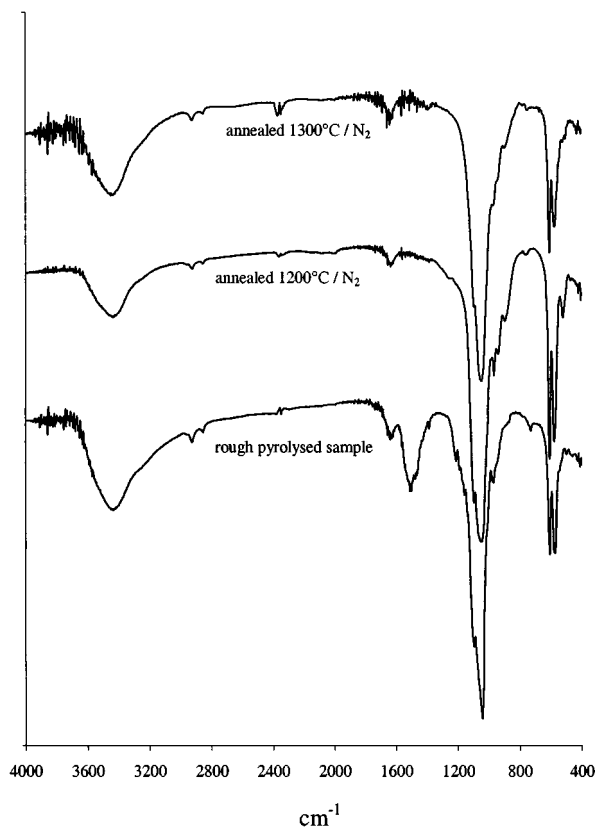


Figure 5 Infrared spectra of $\text{Ca}_{9.2}\text{Nd}_{0.8}(\text{PO}_4)_{5.2}(\text{SiO}_4)_{0.8}\text{F}_{1.8}\text{O}_{0.1}\square_{0.1}$ britholite after annealing at different temperatures for 1 hour.

refinement localizes this element preferentially on II sites which border the channels. A similar observation has already been reported from a single crystal of $\text{Ca}_{9.2}\text{Nd}_{0.8}(\text{PO}_4)_{5.1}(\text{SiO}_4)_{0.9}\text{F}_{1.5}\text{O}_{0.25}\square_{0.25}$ [23]. For a rare earth element such as neodymium, it is admitted that it prefers site II of the

calcium phosphate fluorapatite [24]. Lattice parameters of this britholite ($a = 9.3982(2) \text{ \AA}$ and $c = 6.9060(2) \text{ \AA}$) agree well with those of the single crystal quoted above ($a = 9.3998(8) \text{ \AA}$ and $c = 6.9010(5) \text{ \AA}$), which reflects the fact that the formulae of these compounds are nearly identical. As we have reported in the introduction, this identity is in favor of use of the spray pyrolysis technique for preparing such products: the single crystal was obtained by heating at 1700°C [11, 23].

The infrared spectra of this britholite are given in Fig. 5 as a function of the temperature of the annealing treatment. The spectrum of the rough sample shows several bands attributed to the following functions: CO_3^{2-} (broad band around $1400\text{--}1500 \text{ cm}^{-1}$), PO_4^{3-} ($570, 604, 966, 1042, 1094 \text{ cm}^{-1}$), SiO_4^{4-} (shoulder around $900\text{--}950 \text{ cm}^{-1}$) and SiO_2 (727 cm^{-1} , shoulder about $1150\text{--}1210 \text{ cm}^{-1}$) [25–27]. An annealing treatment at 1000°C (not represented) and 1200°C lead to the disappearance of carbonate ions and SiO_2 and to an increase of the intensity of the ortho-silicate group, SiO_4^{4-} according to the intensity of PO_4^{3-} groups. In this case, the infrared observations, transformation of SiO_2 into SiO_4^{4-} , are more convenient than XRD ones to determine the purity of a product. Let us recall that the XRD of the rough sample presents poorly crystallized apatite. Thus silica must be in an amorphous state, as is often the case [28]. The infrared spectrum of the sample heated at 1300°C is practically the same as the one of the sample heated at 1200°C .

The SEM micrograph of the rough spray pyrolysed sample is shown on Fig. 6. The distribution of the particles is quite homogeneous. Particles are spherical with a mean diameter size a little bit lower than $1 \mu\text{m}$. Attempts to evaluate the sinterability of this powder are in progress. Rough pyrolysed britholites are too

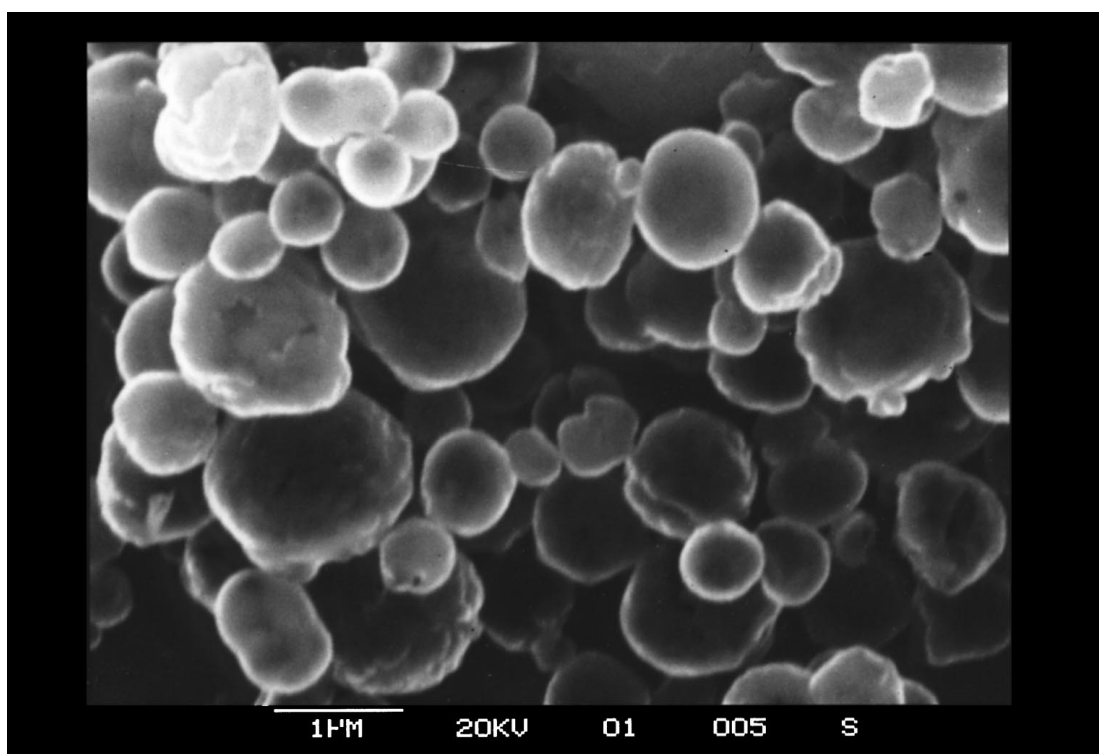


Figure 6 SEM image of a rough spray pyrolysed (1000°C) sample $\text{Ca}_{9.2}\text{Nd}_{0.8}(\text{PO}_4)_{5.2}(\text{SiO}_4)_{0.8}\text{F}_{1.2}\text{O}/\text{OH}/\square_{\text{complement}}$.

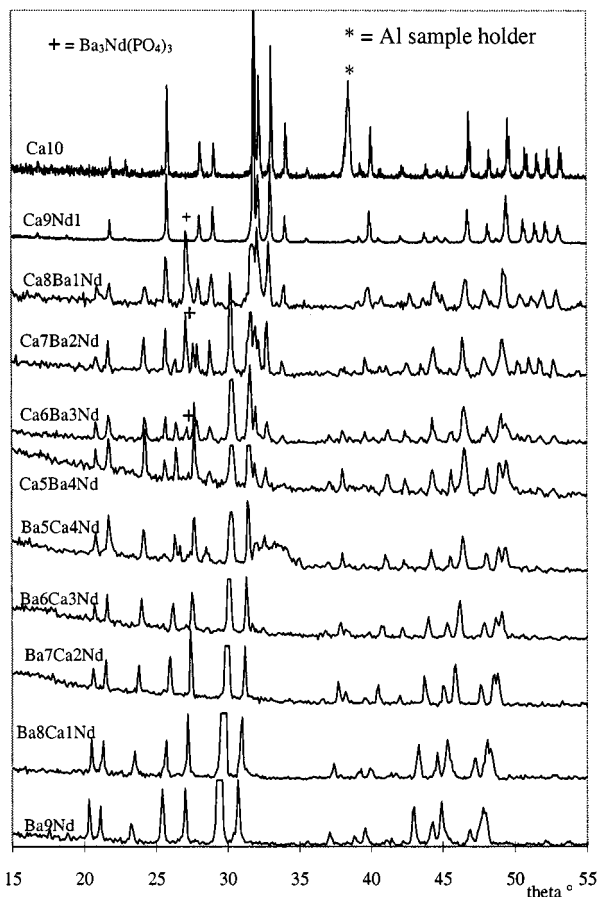


Figure 7 XRD patterns of $\text{Ca}_{9-x}\text{Ba}_x\text{Nd}(\text{PO}_4)_{6-x}(\text{SiO}_4)\text{F}_2$ series (spray pyrolysed at 1000°C and annealed at 1200°C under nitrogen for 1 hour).

porous to be sintered directly. However, a quite soft annealing treatment at 1200°C leads to very well-crystallised submicrometric particles which seem to be easily sinterable.

apatite volume cell (\AA^3)

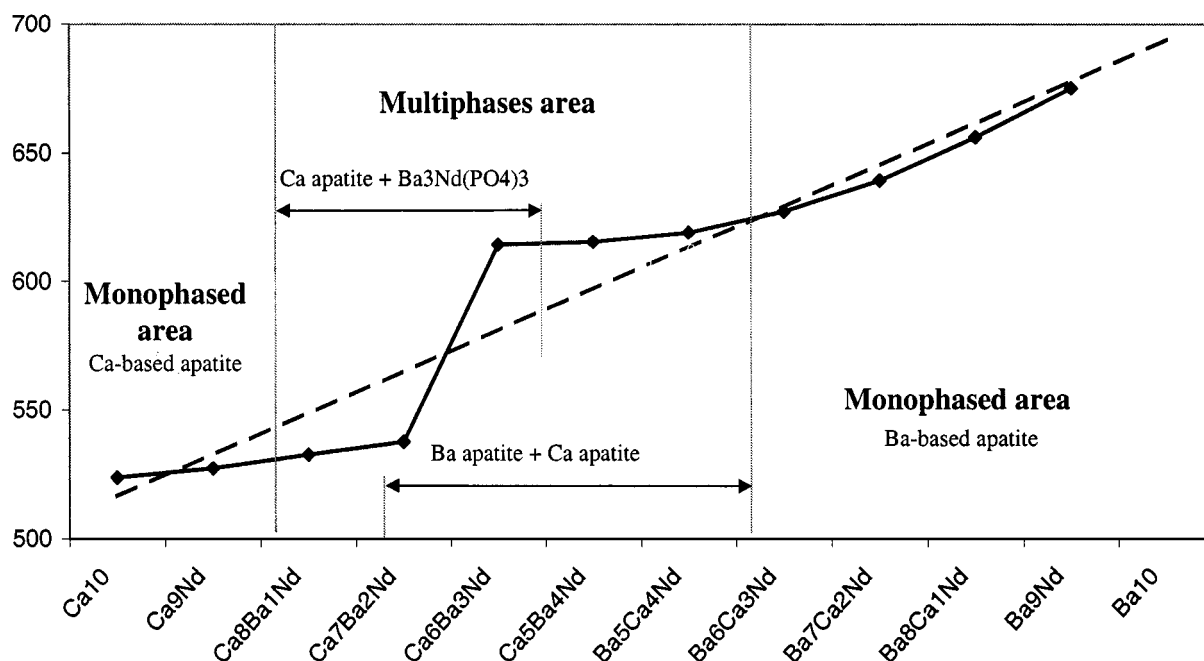


Figure 8 Evolution of the apatite phases cell volume versus the content of barium in $\text{Ca}_{9-x}\text{Ba}_x\text{Nd}(\text{PO}_4)_{6-x}(\text{SiO}_4)\text{F}_2$ series (spray pyrolysed at 1000°C and annealed at 1200°C under nitrogen for 1 hour).

3.2.2. Study of the solid solution, $\text{Ca}_{9-x}\text{Ba}_x\text{Nd}(\text{PO}_4)_{6-x}(\text{SiO}_4)\text{F}_2$

As reported in the introduction, some compounds based on barium phosphate appear well suited for actinide confinement [29]. This is the reason why we studied the barium substitution in the previous calcium britholite. In the case of phosphate hydroxyapatite, obtained in aqueous medium, only a part of the solid solution between calcium and barium was shown to exist. This solid solution appears in a range from 60 to 100% at. of barium atom [30].

The starting reactants always contained an excess of fluoride ions ($\text{F}^-/(\text{PO}_4)^{3-} + (\text{SiO}_4)^{4-} = 3$). The rough samples were annealed for one hour at 1200°C under a stream of nitrogen. XRD patterns of all the compounds with $0 \leq x \leq 9$ are presented in Fig. 7. For the sake of clarity, some of the main peaks have been scaled down to show the lowest intensity peaks.

For $x = 1$, two phases are present: apatite and a barium-neodymium phosphate, $\text{Ba}_3\text{Nd}(\text{PO}_4)_3$ (JCPDS card 26-0194). The apatite peaks are a bit wider than for $x = 0$ and a slight shift of the peaks occurs between the two values of x .

For $2 \leq x \leq 3$, the barium-neodymium phosphate phase as well as the apatite phase previously observed decrease and the intensities of several additional peaks increase: these latter peaks can be attributed to an apatite which will contain elemental barium rather than elemental calcium.

For $4 \leq x \leq 5$, the mixed phosphate phase has completely disappeared, and the intensity of the two apatite phases vary in opposite directions: barium apatite increases while calcium apatite decreases.

Finally for $6 \leq x \leq 9$, XRD patterns show the presence of one apatite phase with a peak shift practically proportional to x .

Such a shift appears more clearly in Fig. 8, which presents the volume of the apatite as a function of x . For $6 \leq x \leq 9$, this volume is close to the Vegard's law line, which is represented by a dotted line. When the two apatite phases are simultaneously present ($5 \geq x \geq 3$), the volume of the barium apatite tends to some asymptotic limit. In the case of calcium apatite, the introduction of one or two barium atoms results in a slight increase of volume, but the increase is less than the corresponding one of the Vegard's law line. But the resulting apatite is mixed with some mixed-metal phosphate.

The lower barium substitution limit in the apatite formula corresponds to $x = 6$. It is worthwhile noticing that, in the apatite structure, this last value corresponds to an entire occupancy of one site (cationic site II). This would be in favor of preferential localization of the barium atoms on these sites. It is known that the respective volume of the two cationic sites greatly differs [31, 32]: the volume of site I being greater (around 38%) than that of site II. Knowing that the radius of barium(II) is much larger the radius of calcium(II) ($r_{\text{Ba}^{2+}} = 1.42 \text{ \AA}$; $r_{\text{Ca}^{2+}} = 1.12 \text{ \AA}$, [33]), we conclude it will not be convenient to localize the barium in the less bulky site. Besides, several works have concluded that the barium element occupied site II in mixed apatites [34, 35].

It is also noticeable, although we were unable to prepare barium-based pure phosphate apatite (both Hap and Fap), that barium britholite can be synthesized without any difficulties. Thus we can conclude the substitution of one phosphate group by a silica one is very beneficial for the stability of the barium apatite structure.

4. Conclusion and perspectives

Even if pure calcium hydroxyapatite cannot be obtained by the spray pyrolysis method, fluorapatite and more particularly britholite with a composition close to $\text{Ca}_9\text{Nd}(\text{PO}_4)_5(\text{SiO}_4)\text{F}_2$ can be easily synthesised at relatively low temperature using that spray pyrolysis apparatus. This technique is a quasi-continuous elaboration process which could be adapted without too many difficulties in the nuclear industry. The particular britholite composition including five phosphate groups for one silicate group probably would play a strategic role in the near future for minor actinides' (Am, Cm, Np) confinement because it seems to be the best balance between a low solubility (given by silicate and fluoride anions) and a high resistance to irradiation damage (given by phosphate group) [4]. Thus, the next challenge is to produce several kilograms of a final material, including minor actinide, to test it as near as possible to the real storage condition.

Substitution of elemental calcium by barium has another goal: the confinement of the volatile fissionogenic products, which are respectively ^{129}I and ^{135}Cs . Up to now these two very bulky radioactive nucleids cannot be easily stored in any matrix. Indeed, the biggest problems with these two elements are due to their volatility and their size. To fix them both inside a mineral matrix, it is necessary to find an host material which will accept such bulky anions or cations in their structure

using an exchange process working at low temperature. Rough spray pyrolysed apatites, since they are very porous, probably will present very interesting exchange properties but preliminary attempts have shown that the calcium fluorapatite structure is not able to incorporate noticeable proportions of $^{129}\text{I}^-$ and $^{135}\text{Cs}^+$ ions. Thus, we put much hope in barium-based apatite, but this is another story that we will present in another paper.

References

1. See for example *La Recherche* n°301 (1997) 63.
2. J. CARPENA and J. L. LACOUT, *Actual. Chim.* **2** (1997) 3.
3. R. GUILLAUMONT, *ibid.* **8/9** (1997) 4.
4. Workshops of Groupement de Recherche "Nomade," Aix en Provence, 3 and 4 Mars 1999; Toulouse, 9 Juillet 1999; Lyon, 9 Septembre 1999.
5. R. C. EWING, W. LUTZE and W. J. WEBER, *J. Mater. Res.* **10** (1995) 243.
6. W. J. WEBER, R. C. EWING and A. MELDRUM, *ibid.* **250** (1997) 147.
7. R. BODUR, H. BOUZIGUES, N. MORIN and J. P. PFIFFELMANN, *C. R. Acad. Sci. Paris* **1731** (1972) 275.
8. J. C. ELLIOTT, in "Structure and Chemistry of the Apatites and other Calcium Orthophosphate" (Elsevier, Amsterdam, The Netherlands, 1994).
9. C. REY, *l'Act. Chim.* **7** (1995) 41.
10. E. R. KREIDLER, Ph.D. Thesis, The Pennsylvania State University, 1967.
11. L. BOYER, Ph.D. Thesis, Institut National Polytechnique, Toulouse, 1997.
12. L. BOYER, J. L. LACOUT and J. CARPENA, *Solid State Ionics* **95** (1997) 121.
13. S. INOUE and A. ONO, *J. Ceram. Soc.* **95** (1987) 759.
14. K. ITATANI, O. TAKAHASHI, A. KISHIOKA and M. KINOSHITA, *Gypsum & Lime* **213** (1988) 19.
15. M. AIZAWA, K. ITATANI, F. S. HOWELL and A. KISHIOKA, *J. Ceram. Soc. Jpn.* **104** (1996) 126.
16. M. AIZAWA, T. HANAZAWA, K. ITATANI, F. S. HOWELL and A. KISHIOKA, *J. Mater. Sci.* **34** (1999) 2865.
17. J. L. DESCHANVRES, F. CELLIER, G. DELABOUGLISE, M. LABEAU, M. LANGLET and J. C. JOUBERT, *J. Phys. Colloq. C5* **50**(5) (1989) 695.
18. Methanol is added to decrease the solution surface strain and thus to increase the atomisation yield.
19. S. AMRAH BOUALI, Ph.D. Thesis, Institut National Polytechnique, Toulouse, 1993.
20. J. C. TROMBE, Thèse d'Etat, Université Paul Sabatier, Toulouse, 1972; *Ann. Chim. (Paris)* 14th Ser. **8** (1973) 335.
21. G. BONEL, Thèse d'Etat, Université Paul Sabatier, Toulouse, 1970.
22. K. A. GROSS, C. C. BERNDT, P. STEPHENS and R. DINNEBIER, *J. Mater. Sci.* **33** (1998) 3985.
23. L. BOYER, J. M. SAVARIAULT, J. CARPENA and J. L. LACOUT, *Acta Cryst.* **C54** (1998) 1057.
24. M. E. FLEET and Y. PAN, *Am. Miner.* **82** (1997) 870.
25. P. TARTE, Thèse d'Agrégation de l'Enseignement Supérieur, Bruxelles, 1965.
26. K. NAKAMOTO, "Infrared Spectra of Inorganic and Coordination Compounds," 2nd ed. (J. Wiley & Sons, New York, 1970).
27. S. D. ROSS, "Inorganic Infrared and Raman Spectra" (McGraw-Hill Book Company, London, 1972).
28. A. MOSSET, P. BAULES, P. LECANTE, J. C. TROMBE, H. AHAMDANE and F. BENSAMKA, *J. Mater. Chem.* **6** (1996) 1527.
29. A. GUESDON and B. RAVEAU, *Chem. Mater.* **10** (1998) 3471.
30. A. BIGI, E. FORESTI, F. MARCHETTI, A. RIPAMONTI and N. ROVERTI, *J. Chem. Soc. Dalton Trans.* (1984) 1091.

31. J. C. ELLIOTT, Ph.D. Thesis, London, 1964.
32. R. A. YOUNG, in Comptes Rendus du Colloque International du CNRS, "Physicochimie et Cristallographie des Apatites d'intérêt biologique" Paris, 10–15 Septembre 1973, p. 21.
33. R. D. SHANNON and C. T. PREWITT, *Acta Cryst.* **B25** (1969) 925.
34. V. S. URUSOV and V. O. KHUDOLOZHKIN, *Geochem. Inter.* **10** (1974) 1059.
35. *Idem.*, *ibid.* **11** (1975) 1048.

*Received 22 March
and accepted 4 October 2000*